

---

# Unsupervised Progressive Learning and the STAM Architecture

---

James Smith<sup>1</sup> Seth Baer<sup>\*1</sup> Cameron Taylor<sup>\*1</sup> Constantine Dovrolis<sup>1</sup>

## Abstract

We first pose the Unsupervised Progressive Learning (UPL) problem: learning salient representations from a non-stationary stream of unlabeled data in which the number of object classes increases with time. To solve the UPL problem we propose an architecture that involves a module called Self-Taught Associative Memory (STAM). Layered hierarchies of STAM modules learn based on a combination of online clustering, novelty detection, forgetting outliers, and storing only prototypical representations rather than specific examples. We evaluate STAM representations using clustering and classification tasks, relying on limited labeled data for the latter. Even though there are no prior approaches that are directly applicable to the UPL problem, we compare the STAM architecture to a couple of unsupervised and self-supervised deep learning approaches adapted in the UPL context.

## 1. Introduction

We start by posing a challenging problem, referred to as *Unsupervised Progressive Learning (UPL)* (see Figure 1). In UPL, the agent observes a sequence (or stream) of unlabeled data vectors  $\{\mathbf{x}_t\}_{t \in \mathbb{N}}$  with  $\mathbf{x}_t \in \mathbb{R}^n$ . Each vector  $\mathbf{x}_t$  is associated with a class  $k(x_t)$  and the vectors of class  $k$  follow a distribution  $F_k$ . The class information, however, is hidden from the agent. Occasionally, the agent may be asked to perform an offline task related to the representations learned from the data stream. For example, the agent may be asked to cluster some unlabeled query vectors into  $k^*$  classes. Or, the agent may be given a small number of labeled examples of one or more classes (to associate “names” with the learned representations), enabling classification tasks. The number of clusters or output classes may stay constant (“persistent tasks”) or increase with time (“expanding tasks”).

<sup>\*</sup>Equal contribution <sup>1</sup>College of Computing, Georgia Institute of Technology, Atlanta, GA. Correspondence to: Constantine Dovrolis <constantine@gatech.edu>.

We denote as  $U_t$  the set of hidden class labels the agent has seen up to time  $t$ . This set is gradually increasing, meaning that the agent progressively learns about more classes. In the UPL context, the goal is to learn in an online manner salient representations of the unlabeled input stream so that the agent can, at any point in time  $t$ , perform unsupervised, supervised, or semi-supervised tasks based on the representations it has learned so far. We require an online learner for pragmatic reasons: it would not be possible or desirable in practice to store and/or process all previously seen data. The online nature of the problem constrains the solution space: methods that require multiple passes over the training data and/or IID sampled minibatches are not applicable in the UPL context.

We assume that the distribution  $F_k$  associated with class  $k$  may also change with time – but this is a slow and gradual process so that an online learner can track changes in  $F_k$ . Abrupt changes would require that the agent forgets what was previously learned about class  $k$  – we do not consider that possibility in this paper.

We do not add any further constraints on the structure of the data sequence. For instance, it is possible that the learner first observes a labeled example of class  $k$  at time  $t$  even though it has not seen any unlabeled examples of that class prior to  $t$  (i.e.  $k \notin U_t$ ) – this requires a transfer-learning capability so that the learner can identify class  $k$  based on representations it has previously learned from other classes. Another interesting scenario is when the unlabeled data arrive in separated class phases, which are unknown to the agent, so that each phase includes data from only few new classes. This is a challenging task from the perspective of catastrophic forgetting because the learner should not forget previously learned classes for which it does not see any new examples. We consider such UPL scenarios in Section 6.

It is plausible that UPL represents how animals learn, at least in the case of *perceptual learning* (Goldstone, 1998): they observe their environment, which is predominantly “unlabeled”, and so they learn to gradually distinguish between a growing number of different object categories even when they do not yet have a way to name them. Later, some of those classes may be associated with words (in the case of humans) (Ashby & Maddox, 2005), or more generally,

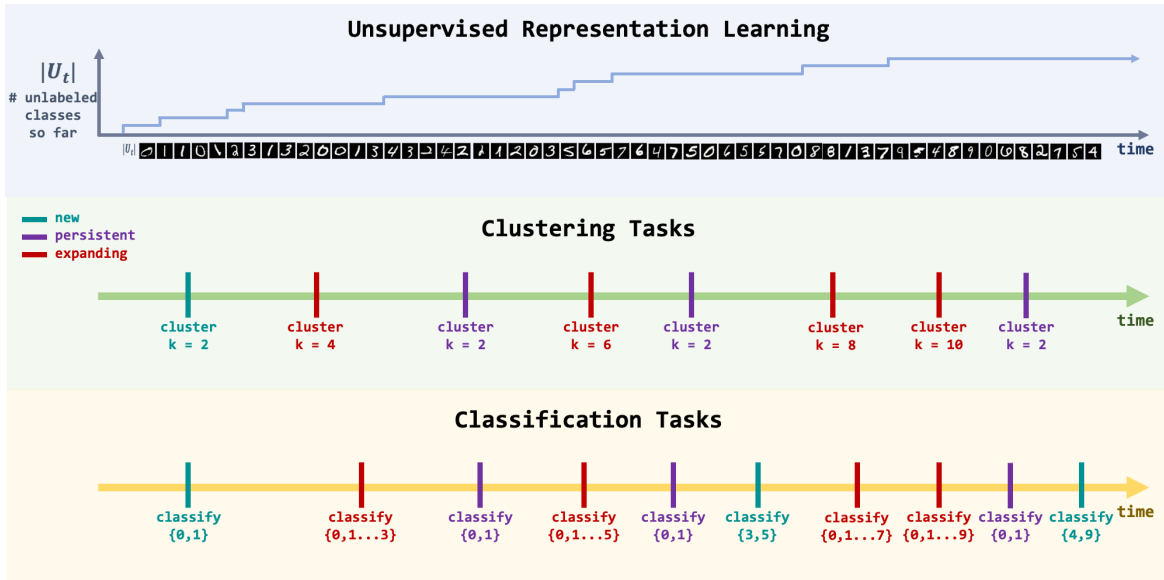


Figure 1. In the UPL problem, the agent observes a stream of unlabeled data in which the number of classes increases with time. The agent has to learn representations that distinguish the classes seen so far, without catastrophic forgetting and without the replay of previously seen data. At any time, the agent may be asked to perform clustering, classification or other tasks using the representations it has learned so far.

with a specific taste, odor, reward, fear, etc. (Watanabe et al., 2001).

## 2. Related Work

The UPL problem has some similarities with several recent approaches in the machine learning literature but it is also different from them in important aspects we describe in this section. Each paragraph highlights the most relevant prior work and explains how it is different from UPL.

**I. Unsupervised learning:** There have been great strides in representation learning methods (Bengio et al., 2013) via clustering (Caron et al., 2018; Jiang et al., 2017a; Xie et al., 2016; Yang et al., 2016), generative models (Eslami et al., 2016; Jiang et al., 2017b; Kosiorek et al., 2018; 2019), information theory (Hjelm et al., 2019; Ji et al., 2019), among others. While such methods can learn representations without data labels, they require prior information about the number of classes present in a given dataset (to set the number of cluster centroids or class outputs) and therefore cannot be directly applied in the UPL setting.

An exception is autoencoder-based methods, which are compatible with UPL given that they do not require any prior task information (Bengio, 2014; Tschannen et al., 2018; Zhou et al., 2012). Therefore, we compare STAM to an autoencoder baseline in Section 6. Generative-based auto encoders (including variational autoencoders) require repeated data sampling and so they cannot be trained by processing each input example only once (Kingma &

Welling, 2013).

**II. Semi-supervised learning (SSL):** SSL addresses scarcity of labeled data by leveraging large amounts of unlabeled training data (Lee, 2013; Kingma et al., 2014; Miyato et al., 2018; Oliver et al., 2018; Rasmus et al., 2015; Springenberg, 2015; Tarvainen & Valpola, 2017). SSL methods require labeled data during the representation learning stages and are therefore not compatible with the UPL problem – the latter uses labeled data only to associate previously learned representations with class labels in classification tasks.

**VII. Self-Supervised Learning:** These methods require an auxiliary task to extract semantically rich features from exclusively unlabeled data (Doersch et al., 2015; Gidaris et al., 2018; Oord et al., 2018). Because these methods require no labeled data and no information about the downstream task, they are suitable for comparison with UPL. As a baseline method, we have chosen the auxiliary task of predicting image rotations (Gidaris et al., 2018). This task is chosen because it has a stable loss function and it does not require data replay.

**III. Few-shot learning (FSL) and Meta-learning:** Such methods recognize object classes not seen in the training set with only a single (or handful) of labeled examples (Fei-Fei et al., 2006; Finn et al., 2017; Ren et al., 2018; Snell et al., 2017). Similar to SSL, FSL methods require labeled data to learn representations and therefore are not applicable in the UPL context. Centroid networks (Huang et al., 2019) do

not require labeled examples at inference time but require labeled examples for training.

**IV. Multi-Task Learning (MTL):** Any MTL method that involves separate heads for different tasks is not compatible with UPL because task boundaries are not known a priori in the UPL scenario (Ruder, 2017). MTL methods that require pre-training on a large labeled dataset are also not applicable to UPL (Pan & Yang, 2010; Yosinski et al., 2014).

**V: Continual learning (CL):** CL approaches aim to mitigate catastrophic forgetting (Goodfellow et al., 2013; Hsu et al., 2018; Parisi et al., 2019; van de Ven & Tolias, 2019) during a sequence of tasks with known boundaries. CL methods can largely be separated into regularization-based approaches (Aljundi et al., 2018; Golkar et al., 2019; Hayes & Kanan, 2019; Kirkpatrick et al., 2017; Yoon et al., 2018; Zenke et al., 2017) or distillation-based methods (Li & Hoiem, 2017), and replay-based methods (Chaudhry et al., 2019a;b; Gepperth & Karaoguz, 2017; Hayes et al., 2019; Kemker et al., 2018; Kemker & Kanan, 2018; Lopez-Paz & Ranzato, 2017; Rebuffi et al., 2017; Shin et al., 2017) which require stored or generated examples. Because these methods require known task boundaries and/or stored/generated examples, they are not directly applicable in the UPL context.

There is some limited work that does not require known task boundaries or stored/generated examples but still requires labeled data (Aljundi et al., 2019; Zeno et al., 2018). The most similar work to UPL is the Continual Unsupervised Representation Learning (CURL) scheme (Rao et al., 2019), which also learns data representations without knowledge of task identity. However, CURL relies on extensive data replay, which is not allowed in UPL. Crucially, CURL also assumes knowledge of the number of classes present in the given tasks.

**VI. Online Sequence Learning and Progressive Learning:** Many approaches learn in an online manner, meaning that data is processed in fixed batches and discarded afterwards. One area of online learning is continuous online sequence learning. A comparison of these methods, including the Hierarchical Temporal Memory model, was conducted by Cui et al. (Cui et al., 2016). These methods however do not address the UPL problem. Another group of online methods is progressive learning, where a supervised classification model must be able to learn in an online manner without prior knowledge of the number of classes (Rusu et al., 2016; Venkatesan & Er, 2016). The existing approaches in this area however require supervision whenever a new class appears. There are also approaches in the data streaming literature involving limited supervision (Chiotellis et al., 2018; Li et al., 2018; Loo & Marsono, 2015) but they require labeled data in the training stream.

### 3. Representation Learning and STAM Architecture

The learning approach that we pursue in this work is based on online clustering, novelty detection, separate short-term and long-term memories, and storing only prototypical representations rather than specific examples. In the following, we describe the STAM architecture as a sequence of its major components.

The notation is summarized for convenience in the Supplementary Material section SM-A. The image preprocessing pipeline is minimal and is described in SM-G.

**I. Hierarchy of increasing receptive fields:** An input vector  $\mathbf{x}_t \in \mathbb{R}^n$  (an image in all subsequent examples) is analyzed through a hierarchy of  $\Lambda$  layers. Instead of neurons or hidden-layer units, each layer consists of STAM units – in its simplest form a STAM unit functions as an online clustering module. Each STAM processes one  $\rho_l \times \rho_l$  patch (subvector) of the input at that layer. The patches are overlapping, with a small stride (set to one pixel in our experiments), to accomplish translation invariance (similar to CNNs). The patch dimension  $\rho_l$  increases in higher layers – the idea is that the first layer learns the smallest and most elementary patterns while the top layer learns the largest and most complex patterns.

**II. Online clustering:** Every patch of each layer is clustered, in an online manner, to a set of centroids. These time-varying centroids form the *prototypical patterns* that the STAM architecture gradually learns at that layer. All STAM units of layer  $l$  share the same set of centroids  $C_l(t)$  – again for translation invariance.<sup>1</sup> Given the  $m$ 'th input patch  $\mathbf{x}_{1,m}$  at layer  $l$ , the nearest centroid of  $C_l$  selected for  $\mathbf{x}_{1,m}$  is

$$\mathbf{c}_{1,j} = \arg \min_{\mathbf{c} \in C_l} d(\mathbf{x}_{1,m}, \mathbf{c}) \quad (1)$$

where  $d(\mathbf{x}_{1,m}, \mathbf{c})$  is the Euclidean distance between the patch  $\mathbf{x}_{1,m}$  and centroid  $\mathbf{c}$ .<sup>2</sup> The selected centroid is updated based on a learning rate parameter  $\alpha$ , as follows:

$$\mathbf{c}_{1,j} = \alpha \mathbf{x}_{1,m} + (1 - \alpha) \mathbf{c}_{1,j}, \quad 0 < \alpha < 1 \quad (2)$$

A higher  $\alpha$  value makes the learning process faster but less predictable. We do not use a decreasing value of  $\alpha$  because the goal is to keep learning in a non-stationary environment rather than convergence to a stable centroid. If the centroid  $\mathbf{c}_{1,j}$  is selected by more than one patches of the same input, the centroid is updated based on the closest patch to that centroid.

An online clustering algorithm that is similar to our ap-

<sup>1</sup>We drop the time index  $t$  from this point on but it is still implied that the centroids are dynamically learned over time.

<sup>2</sup>We have also experimented with the L1 distance metric with only minimal differences.

proach (and asymptotically equivalent to k-means) can be implemented with a simple recurrent neural network of excitatory and inhibitory spiking neurons using strictly Hebbian learning, as shown recently (Pehlevan et al., 2017).

**III. Novelty detection:** When an input patch  $\mathbf{x}_{l,m}$  at layer  $l$  is significantly different than all centroids at that layer (i.e., its distance to the nearest centroid is a statistical outlier), a new centroid is created in  $C_l$  based on  $\mathbf{x}_{l,m}$ . We refer to this event as *Novelty Detection (ND)*. This function is necessary so that the architecture can learn centroids associated with new classes after they appear in the unlabeled data stream.

To do so, we estimate in an online manner the distribution of the Euclidean distance between input patches and their nearest centroid (separately for each layer). We sample a randomly chosen patch from each input vector, only considering the last 1000 inputs. The novelty detection threshold at layer  $l$  is denoted by  $\bar{D}_l$  and it is defined as the 95-th percentile ( $\beta = 0.95$ ) of the distance distribution.

**IV. Dual-memory organization:** New centroids are stored temporarily in a *Short-Term Memory (STM)* of limited capacity  $\Delta$  (separate for each layer). Every time a centroid is selected as the nearest neighbor of an input patch, it is updated based on (2). If an STM centroid  $\mathbf{c}_{l,j}$  is selected  $s_{l,j} > \theta$  times, it is copied to the *Long-Term Memory (LTM)* for that layer. We refer to this event as *memory consolidation*. The LTM has (practically) unlimited capacity and the learning rate is much smaller (in our experiments, set to zero).

This memory organization is inspired by the Complementary Learning Systems framework (Kumaran et al., 2016), where the STM role is played by the hippocampus and the LTM role by the cortex. This dual-memory scheme is necessary to distinguish between infrequently seen patterns that can be forgotten, and new patterns that are frequently seen after they first appear.

We initialize the pool of STM centroids at each layer using randomly sampled patches from the unlabeled stream (a single patch from each image to maximize diversity).

When the STM pool of centroids at a layer is full, the introduction of a new centroid (created through novelty detection) causes the removal of an earlier centroid. We use the Least-Recently Used (LRU) policy to remove atypical centroids that have not been recently selected by any input. Figure 2 illustrates this dual-memory organization.

**V. A note about clustering-based methods:** Even though clustering has been used successfully in the past for representation learning (Coates et al., 2011; Coates & Ng, 2012), its effectiveness gradually drops as the input dimensionality increases (Beyer et al., 1999; Hinneburg et al., 2000).

In the STAM architecture, we avoid this issue by clustering smaller subvectors (patches) of the input data. If those subvectors are still of high dimensionality, another approach is to reduce the *intrinsic dimensionality* of the input data at each layer by reconstructing that input using representations (selected centroids) from the previous layer – we have experimented with this approach but not included it here because it is not required in the datasets and tasks we consider in this paper.

## 4. Classification using STAM

Given a small amount of labeled data, STAM representations can be evaluated with an offline classification task.

**I. Associating centroids with classes:** Suppose that we have seen some labeled examples  $X_L(t)$  from a set of classes  $L(t)$  at time  $t$ . In the UPL context, we only use such labeled examples to associate existing LTM centroids at time  $t$  (learned strictly from unlabeled data) with the set of classes in  $L(t)$ .

Given a labeled example of class  $k$ , suppose that there is a patch  $\mathbf{x}$  in that example for which the nearest centroid is  $\mathbf{c}$ . That patch contributes the following association between centroid  $\mathbf{c}$  and class  $k$ :

$$f_{\mathbf{x},\mathbf{c}}(k) = e^{-d(\mathbf{x},\mathbf{c})/\bar{D}_l} \quad (3)$$

where  $\bar{D}_l$  is a normalization constant (calculated as the average distance between input patches and centroids).

The *class-association vector*  $\mathbf{g}_{\mathbf{c}}$  between centroid  $\mathbf{c}$  and any class  $k$  is computed aggregating all such associations, across all labeled examples in  $X_L$ :

$$g_{\mathbf{c}}(k) = \frac{\sum_{\mathbf{x} \in X_L(k)} f_{\mathbf{x},\mathbf{c}}(k)}{\sum_{k' \in L(t)} \sum_{\mathbf{x} \in X_L(k')} f_{\mathbf{x},\mathbf{c}}(k')}, \quad k = 1 \dots L(t) \quad (4)$$

Note that  $\sum_k g_{\mathbf{c}}(k) = 1$ .

**II. Class informative centroids:** If a centroid is associated with only one class ( $g_{\mathbf{c}}(k) = 1$ ), only labeled examples of that class select that centroid. At the other extreme, if a centroid is equally likely to be selected by examples of any labeled class, ( $g_{\mathbf{c}}(k) \approx 1/|L(t)|$ ), the selection of that centroid does not provide any significant information for the class of the corresponding input.

We identify the centroids that are *Class Informative (CIN)* as those that are associated with at least one class more than expected by chance. Specifically, a centroid  $\mathbf{c}$  is CIN if

$$\max_{k \in L(t)} g_{\mathbf{c}}(k) > \frac{1}{|L(t)|} + \gamma \quad (5)$$

where  $\frac{1}{|L(t)|}$  is the chance term and  $\gamma$  is an additional significance term.

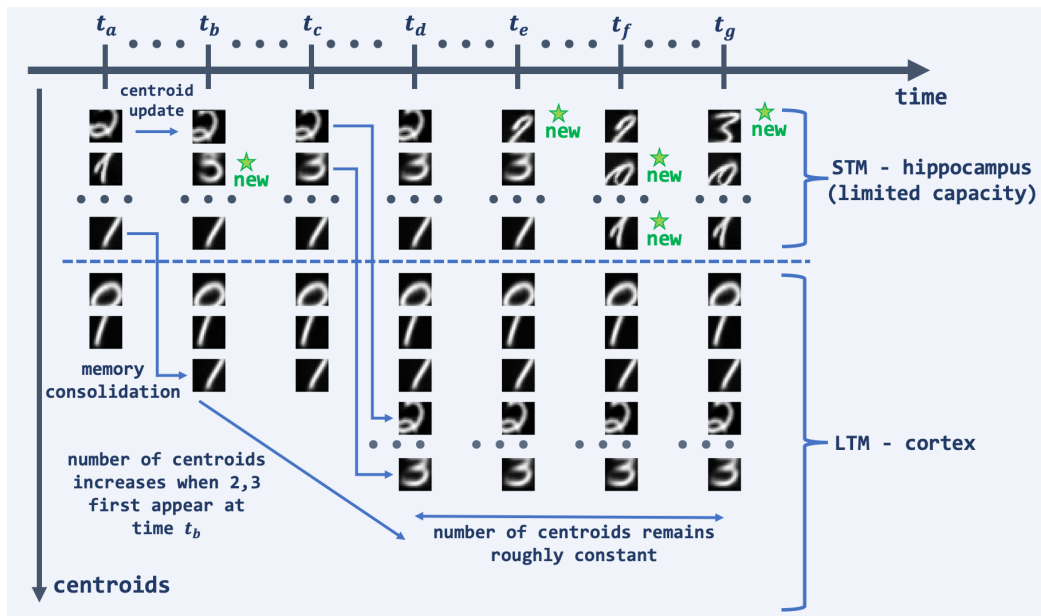


Figure 2. A hypothetical pool of STM and LTM centroids visualized at seven time instants. From  $t_a$  to  $t_b$ , a centroid is moved from STM to LTM after it has been selected  $\theta$  times. At time  $t_b$ , unlabeled examples from classes ‘2’ and ‘3’ first appear, triggering novelty detection and new centroids are created in STM. These centroids are moved into LTM by  $t_d$ . From  $t_d$  to  $t_g$ , the pool of LTM centroids remains the same because no new classes are seen. The pool of STM centroids keeps changing when we receive “outlier” inputs of previously seen classes. Those centroids are later replaced (Least-Recently-Used policy) due to the limited capacity of the STM pool.

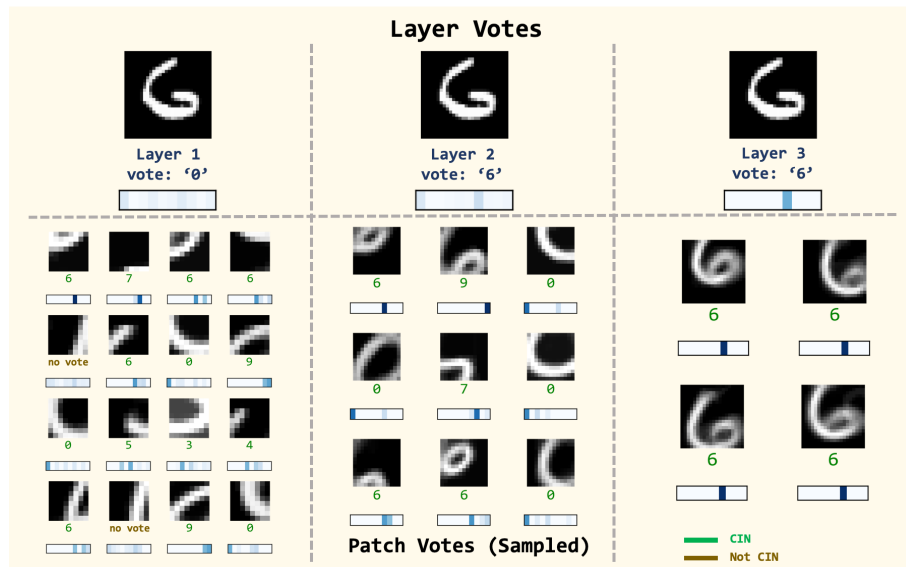


Figure 3. An example of the classification process. Every patch (at any layer) that selects a CIN centroid votes for the single class that has the highest association with. These patch votes are first aggregated at each layer. The final inference is the class with the highest vote across all layers.

**III. Classification using a hierarchy of centroids:** At test time, we are given an input  $\mathbf{x}$  of class  $k(\mathbf{x})$  and infer its class as  $\hat{k}(\mathbf{x})$ . The classification task is a “biased voting” process in which every patch of  $\mathbf{x}$ , at any layer, votes for a single class as long as that patch selects a CIN centroid.

Specifically, if a patch  $\mathbf{x}_{l,m}$  of layer  $l$  selects a CIN centroid  $\mathbf{c}$ , then that patch votes  $v_{l,m}(k) = \max_{k \in L(t)} g_{\mathbf{c}}(k)$  for the class  $k$  that has the highest association with  $\mathbf{c}$ , and zero for all other classes. If  $\mathbf{c}$  is *not* a CIN centroid, the vote of that patch is  $v_{l,m}(k) = 0$  for all classes.

The vote of layer  $l$  for class  $k$  is the average vote across all patches in layer  $l$  (as illustrated in Figure 3):

$$v_l(k) = \frac{\sum_{m \in M_l} v_{l,m}(k)}{|M_l|} \quad (6)$$

where  $M_l$  is the set of patches in layer  $l$ . The final inference for input  $\mathbf{x}$  is the class with the highest cumulative vote across all layers:

$$\hat{k}(\mathbf{x}) = \arg \max_{k'} \sum_{l=1}^{\Lambda} v_l(k) \quad (7)$$

## 5. Clustering using STAM

We can also use STAM representations in unsupervised tasks, such as offline clustering. To do this, we first define an embedding function that maps a given image  $\mathbf{x}$  into the space defined by STAM LTM centroids. In particular, the embedding is defined as  $\Phi(\mathbf{x}) : \mathbb{R}^n \rightarrow \mathbb{R}^{|C_l|}$ , where the element  $j = 1 \dots |C_l|$  of  $\Phi(\mathbf{x})$  is the normalized distance (equation 3) between the LTM centroid  $c_{l,j}$  and its *closest patch* in  $\mathbf{x}$ . If we think of STAM centroids as features, the embedding vector represents how strongly that feature is present anywhere in the given input. The embedding vectors of a given dataset are then clustered offline using  $k$ -means for a given value of  $k$ . Any other clustering algorithm could be used instead.

## 6. Evaluation

To evaluate the STAM architecture in the UPL context, we consider a datastream in which small groups of classes appear in successive *phases*, referred to as **Incremental UPL**. New classes are introduced two at a time in each phase, and they are only seen in that phase. STAMs must be able to both recognize new classes when they are first seen in the stream, and to also remember all previously learned classes without catastrophic forgetting.

We consider two tasks for evaluation of UPL methods: unsupervised clustering and low-labeled classification. The datasets we evaluate on are MNIST (Lecun et al., 1998), EMNIST (balanced split with 47 classes) (Cohen et al.,

2017), and SVHN (Netzer et al., 2011). For each task, we average results over three trials (different unlabeled data streams). In each trial, we have a randomly sampled hold-out set of 1500 images. Then, we sample from the remaining data to form the unlabeled stream. We perform each task five times, using 1000 randomly sampled test images from the hold-out set. So, each result is the average of 15 task evaluations (the plots show mean  $\pm$  standard deviation). All experiments are run on personal computers.

The STAM results use a 3-layer STAM hierarchy – all hyperparameters values are reported in the SM-A. The robustness of the results as we vary these hyperparameter values is shown in SM-E.

### 6.1. Baseline Methods

Even though there are no prior approaches that are directly applicable in the UPL context, we compare the STAM architecture to a couple of unsupervised and self-supervised deep learning approaches adapted in the UPL context. To be consistent with UPL, the number of training epochs is set to one, and images are processed one at a time. This is necessary so that each unlabeled example is processed only once. Deep learning methods become weaker in this streaming scenario because they cannot train iteratively over several epochs on the same dataset.

The first baseline is a convolutional autoencoder (CAE) architecture trained to optimize Euclidean reconstruction error – see Table SM-5. It is trained using Adam optimization (Kingma & Ba, 2014) with a learning rate of  $1^{-4}$  and no decay. The encoder consists of three convolution layers with ReLU activations, embedding inputs into a 64-dimension latent space. The decoder consists of three transposed convolution layers with ReLU activations. The final layer uses linear activations. The representations at the 64-dimension latent space are used to perform the clustering and classification tasks.

The second baseline is a self-supervised method based on rotations (RotNet), (Gidaris et al., 2018). The training data is augmented so that each training image is rotated by 0, 90, 180 and 270 degrees. The network is trained by minimizing the cross-entropy loss on a four-way classification task of predicting the rotation of the training images. The model uses a *network-in-network* architecture with five *conv-blocks*, where each conv-block consists of three convolutional layers. We train the network with SGD with a batch size of 4 (the four rotations of a single training image in the original data set) and with one epoch, again to only process each unlabeled example once. The momentum is set to 0.9 and the learning rate to 0.1. In order to perform clustering and classification we generate a feature map from the outputs of the network’s second conv-block, which produces the best features for downstream tasks ac-

ording to (Gidaris et al., 2018).

For both baselines, the classification task is performed using a  $K$  nearest-neighbor (KNN) classifier – we have experimented with various values of  $K$  and other single-pass classifiers, and report only the best performing baseline results here.

## 6.2. Classification Task

The classification task that we focus on in the Incremental UPL case is *expanding*, meaning that in each phase we need to classify *all* classes seen so far. Given a few labeled examples for the classes that have been present in the stream up to time  $t$ , the algorithm is asked to perform object classification on testing data.

The results of the classification task are given in Figure 4. As we introduce new classes to the incremental UPL stream, the average accuracy per phase decreases for all methods in each dataset. This is expected, as the task gets *more difficult* after each phase. We focus on which method performs best in each task, and which methods see a smaller decrease in accuracy per phase. In the first dataset (MNIST), we observe that STAM performs consistently better than RotNet and CAE, and STAM is less vulnerable to catastrophic forgetting. For SVHN, the trend is similar after the first phase but the difference between STAM and RotNet is much smaller. Finally, in EMNIST, we see a consistently higher accuracy with STAM compared to the deep learning baselines.

## 6.3. Clustering Task

For the clustering task, we report an accuracy metric that is calculated using the test data labels (that information is *not* used in representation learning or clustering). Given that we have the same number of test vectors per class, we associate each cluster with the most-represented class in that cluster. Any instances of another class in that cluster are counted as errors. The number of clusters  $k$  is equal to the number of classes seen up to that phase in the unlabeled datastream.

The results of the clustering task are given in Figure 5. For MNIST, STAM still performs consistently better than the two other methods, and its accuracy stays almost constant going from 4 classes to 10 classes. For SVHN, RotNet performs significantly better. Finally, for EMNIST, STAM outperforms the two deep learning methods without experiencing significant loss of accuracy after the first 10 phases (20 classes).

## 6.4. STAM Ablations

Several STAM ablations are presented in Figure 6. On the left, we remove the LTM capabilities and only use STM centroids for classification. During the first two phases, there is little (if any) difference in classification accuracy. However, we see a clear dropoff during phases 3-5. This suggests that, without the LTM mechanisms, patterns from classes that are no longer seen in the stream are forgotten over time, and STAMs can only successfully classify classes that have been recently seen.

We also investigate the importance of having static LTM centroids rather than dynamic centroids (center). Specifically, we replace the static LTM with a dynamic LTM in which the centroids are adjusted with the same learning rate parameter  $\alpha$ , as in STM. The accuracy suffers drastically because the introduction of new classes “takes over” LTM centroids of previously learned classes, after the latter are removed from the stream. Similar to the removal of LTM, we do not see the effects of “forgetting” until phases 3-5. Note that the degradation due to a dynamic LTM is less severe than that from removing LTM completely.

Finally, we look at the effects of removing layers from the STAM hierarchy (right). We see a small drop in accuracy after removing layer 3, and a large drop in accuracy after also removing layer 2. The importance of having a deeper hierarchy would be more pronounced in datasets with higher-resolution images or videos, potentially showing multiple objects in the same frame. In such cases, CIN centroids can appear at any layer, starting from the lowest to the highest.

## 6.5. Additional results

The reader can find additional experimental results in the Supp-Material section that focus on the questions: how does the number of LTM centroids increase with time and what fraction of them are “Class Informative” (in classification tasks), how does the accuracy of STAM vary with the number of labeled examples per class, how do the various hyperparameters of the STAM architecture affect classification accuracy, and how does the memory requirement of STAM (to store all centroids) compare to the memory requirement of a baseline deep learning architecture (to store all model parameters)?

## 7. Discussion

We believe that in order to mimic human intelligence, learning methods should be able to learn in a streaming manner and in the absence of supervision. Animals do not “save off” labeled examples to train in parallel with unlabeled data, they do not know how many classes exist in their environment, and they do not have to replay/dream

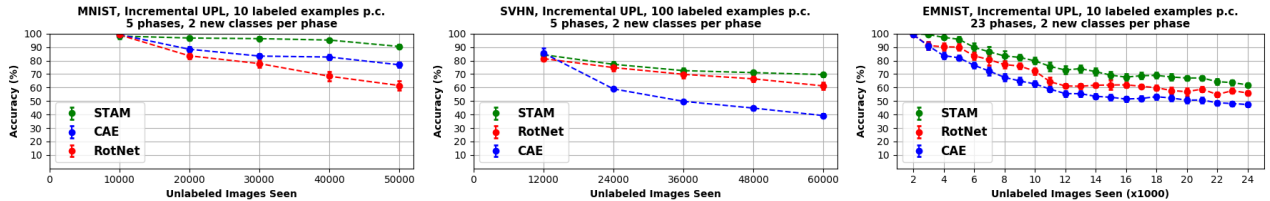


Figure 4. Classification accuracy for MNIST (left), SVHN (center), and EMNIST (right). The task is expanding classification for incremental UPL, i.e., recognize all classes seen so far. Note that the number of labeled examples is 10 per class for MNIST and EMNIST and 100 per class for SVHN.

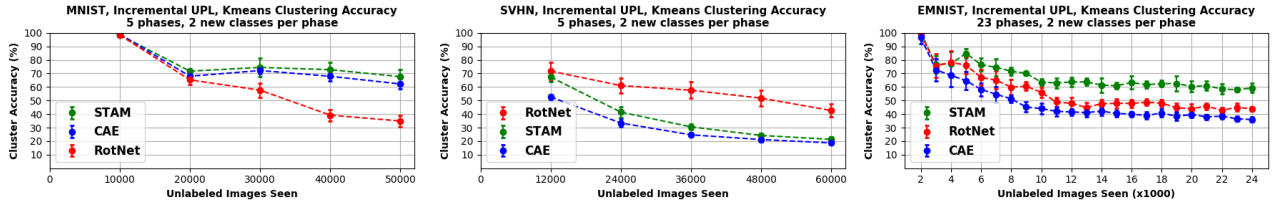


Figure 5. Clustering accuracy for MNIST (left), SVHN (center), and EMNIST (right). The task is expanding clustering for incremental UPL. The number of clusters is equal to the number of classes in the data stream seen up to that point in time.

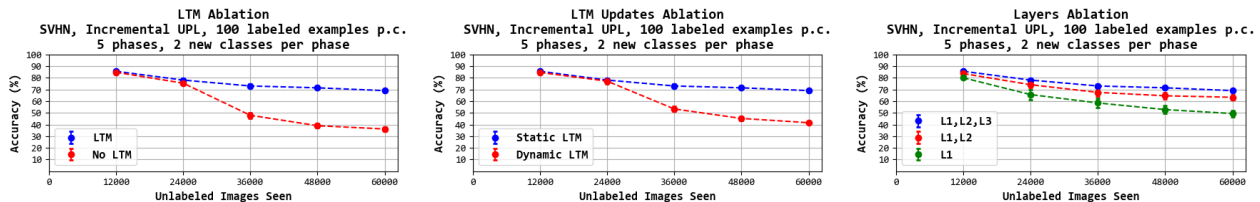


Figure 6. Ablation study: A STAM architecture without LTM (left), a STAM architecture in which the LTM centroids are adjusted with the same learning rate  $\alpha$  as in STM (center), and a STAM architecture with removal of layers (right)

periodically all their past experiences to avoid forgetting them. The proposed STAM architecture aims to address the desiderata that is often associated with Lifelong Learning:

*I. Online learning:* STAMs constantly update their centroids with every example. There is no separate training stage, and there is no specific task for which the network optimizes the features it learns. Any tasks that require classification will of course require one or few labeled examples so that the corresponding clusters that were formed previously are now associated with the name of a class. However, STAMs do not need these labeled examples to learn efficient data representations.

*II. Transfer learning:* The hierarchical nature of the proposed architecture means that features learned (in an unsupervised manner) at lower-level STAMs can be reused in different tasks that higher-level STAMs perform.

*III. Resistance to catastrophic forgetting:* The introduction of a new class or prototype will lead to the creation of

new clusters at some STAMs in the hierarchy (e.g., layer-1 STAMs will learn new elementary visual features if we start feeding them natural images instead of MNIST examples – while a STAM at a higher-level would create a new cluster when it first starts seeing examples of scooters but without affecting the cluster associated with bicycles).

*IV. Expanding learning capacity:* The learning capacity of a STAM architecture depends on two factors: the number of STAMs and the maximum number of centroids that each STAM can store in STM and LTM. The limited capacity constraint in the STM pool requires to forget recently created centroids that have not been recently updated with new examples. The unlimited capacity of the LTM pool of centroids, on the other hand, allows the system to gradually learn an unlimited number of classes, even if it does not see examples of all classes learned earlier.

*V. No direct access to previous experience:* A STAM only needs to store the centroids of the clusters it has learned so far. Those centroids correspond to prototypes, allowing the STAM to generalize. All previously seen exemplars are



discarded.

## Acknowledgements

This work is supported by the Lifelong Learning Machines (L2M) program of DARPA/MTO: Cooperative Agreement HR0011-18-2-0019. The authors acknowledge the comments of Zsolt Kira for an earlier version of this work.

## References

- Aljundi, R., Babiloni, F., Elhoseiny, M., Rohrbach, M., and Tuytelaars, T. Memory aware synapses: Learning what (not) to forget. In *ECCV*, 2018.
- Aljundi, R., Kelchtermans, K., and Tuytelaars, T. Task-free continual learning. In *Proceedings of the IEEE Conference on Computer Vision and Pattern Recognition*, pp. 11254–11263, 2019.
- Ashby, F. G. and Maddox, W. T. Human category learning. *Annu. Rev. Psychol.*, 56:149–178, 2005.
- Bengio, Y. How auto-encoders could provide credit assignment in deep networks via target propagation. *arXiv preprint arXiv:1407.7906*, 2014.
- Bengio, Y., Courville, A., and Vincent, P. Representation learning: A review and new perspectives. *IEEE Trans. Pattern Anal. Mach. Intell.*, 35(8):1798–1828, August 2013. ISSN 0162-8828. doi: 10.1109/TPAMI.2013.50.
- Beyer, K. S., Goldstein, J., Ramakrishnan, R., and Shaft, U. When is "nearest neighbor" meaningful? In *Proceedings of the 7th International Conference on Database Theory, ICDT '99*, pp. 217–235, London, UK, UK, 1999. Springer-Verlag. ISBN 3-540-65452-6.
- Caron, M., Bojanowski, P., Joulin, A., and Douze, M. Deep clustering for unsupervised learning of visual features. In *The European Conference on Computer Vision (ECCV)*, September 2018.
- Chaudhry, A., Ranzato, M., Rohrbach, M., and Elhoseiny, M. Efficient lifelong learning with a-GEM. In *International Conference on Learning Representations*, 2019a.
- Chaudhry, A., Rohrbach, M., Elhoseiny, M., Ajanthan, T., Dokania, P. K., Torr, P. H., and Ranzato, M. Continual learning with tiny episodic memories. *arXiv preprint arXiv:1902.10486*, 2019b.
- Chiotellis, I., Zimmermann, F., Cremers, D., and Triebel, R. Incremental semi-supervised learning from streams for object classification. In *2018 IEEE/RSJ International Conference on Intelligent Robots and Systems (IROS)*, pp. 5743–5749. IEEE, 2018.
- Coates, A. and Ng, A. Y. *Learning feature representations with k-means*, pp. 561–580. Springer, 2012.
- Coates, A., Ng, A., and Lee, H. An analysis of single-layer networks in unsupervised feature learning. In *Proceedings of the fourteenth international conference on artificial intelligence and statistics*, pp. 215–223, 2011.
- Cohen, G., Afshar, S., Tapson, J., and van Schaik, A. Emnist: an extension of mnist to handwritten letters. *ArXiv*, abs/1702.05373, 2017.
- Cui, Y., Ahmad, S., and Hawkins, J. Continuous online sequence learning with an unsupervised neural network model. *Neural Comput.*, 28(11):2474–2504, November 2016. ISSN 0899-7667. doi: 10.1162/NECO\_a\_00893.
- Doersch, C., Gupta, A., and Efros, A. A. Unsupervised visual representation learning by context prediction. *2015 IEEE International Conference on Computer Vision (ICCV)*, pp. 1422–1430, 2015.
- Eslami, S. M. A., Heess, N., Weber, T., Tassa, Y., Szepesvari, D., Kavukcuoglu, K., and Hinton, G. E. Attend, infer, repeat: Fast scene understanding with generative models. In *Proceedings of the 30th International Conference on Neural Information Processing Systems, NIPS'16*, pp. 3233–3241, USA, 2016. Curran Associates Inc. ISBN 978-1-5108-3881-9.
- Fei-Fei, L., Fergus, R., and Perona, P. One-shot learning of object categories. *IEEE Transactions on Pattern Analysis and Machine Intelligence*, 28(4):594–611, April 2006. ISSN 0162-8828. doi: 10.1109/TPAMI.2006.79.
- Finn, C., Abbeel, P., and Levine, S. Model-agnostic meta-learning for fast adaptation of deep networks. In *Proceedings of the 34th International Conference on Machine Learning - Volume 70, ICML'17*, pp. 1126–1135. JMLR.org, 2017.
- Gepperth, A. and Karaoguz, C. Incremental learning with self-organizing maps. *2017 12th International Workshop on Self-Organizing Maps and Learning Vector Quantization, Clustering and Data Visualization (WSOM)*, pp. 1–8, 2017.
- Gidaris, S., Singh, P., and Komodakis, N. Unsupervised representation learning by predicting image rotations. In *International Conference on Learning Representations*, 2018.
- Goldstone, R. L. Perceptual learning. *Annual review of psychology*, 49(1):585–612, 1998.
- Golkar, S., Kagan, M., and Cho, K. Continual learning via neural pruning. *arXiv preprint arXiv:1903.04476*, 2019.

- Goodfellow, I. J., Mirza, M., Xiao, D., Courville, A., and Bengio, Y. An empirical investigation of catastrophic forgetting in gradient-based neural networks. *arXiv preprint arXiv:1312.6211*, 2013.
- Hayes, T. L. and Kanan, C. Lifelong machine learning with deep streaming linear discriminant analysis. *arXiv preprint arXiv:1909.01520*, 2019.
- Hayes, T. L., Cahill, N. D., and Kanan, C. Memory efficient experience replay for streaming learning. In *2019 International Conference on Robotics and Automation (ICRA)*, pp. 9769–9776. IEEE, 2019.
- Hinneburg, A., Aggarwal, C. C., and Keim, D. A. What is the nearest neighbor in high dimensional spaces? In *Proceedings of the 26th International Conference on Very Large Data Bases, VLDB '00*, pp. 506–515, San Francisco, CA, USA, 2000. Morgan Kaufmann Publishers Inc. ISBN 1-55860-715-3.
- Hjelm, D., Fedorov, A., Lavoie-Marchildon, S., Grewal, K., Bachman, P., Trischler, A., and Bengio, Y. Learning deep representations by mutual information estimation and maximization. In *ICLR 2019*. ICLR, April 2019.
- Hsu, Y.-C., Liu, Y.-C., Ramasamy, A., and Kira, Z. Re-evaluating continual learning scenarios: A categorization and case for strong baselines. In *NeurIPS Continual learning Workshop*, 2018.
- Huang, G., Larochelle, H., and Lacoste-Julien, S. Centroid networks for few-shot clustering and unsupervised few-shot classification. *arXiv preprint arXiv:1902.08605*, 2019.
- Ji, X., Henriques, J., and Vedaldi, A. Invariant information clustering for unsupervised image classification and segmentation. In *Proceedings of the International Conference on Computer Vision (ICCV)*, 2019.
- Jiang, Z., Zheng, Y., Tan, H., Tang, B., and Zhou, H. Variational deep embedding: An unsupervised and generative approach to clustering. In *Proceedings of the 26th International Joint Conference on Artificial Intelligence, IJCAI'17*, pp. 1965–1972. AAAI Press, 2017a. ISBN 9780999241103.
- Jiang, Z., Zheng, Y., Tan, H., Tang, B., and Zhou, H. Variational deep embedding: An unsupervised and generative approach to clustering. In *Proceedings of the 26th International Joint Conference on Artificial Intelligence, IJCAI'17*, pp. 1965–1972. AAAI Press, 2017b. ISBN 978-0-9992411-0-3.
- Kemker, R. and Kanan, C. Fearnnet: Brain-inspired model for incremental learning. *International Conference on Learning Representations (ICLR)*, 2018.
- Kemker, R., McClure, M., Abitino, A., Hayes, T., and Kanan, C. Measuring catastrophic forgetting in neural networks. *AAAI Conference on Artificial Intelligence*, 2018.
- Kingma, D. P. and Ba, J. Adam: A method for stochastic optimization. *arXiv preprint arXiv:1412.6980*, 2014.
- Kingma, D. P. and Welling, M. Auto-encoding variational bayes. *arXiv preprint arXiv:1312.6114*, 2013.
- Kingma, D. P., Rezende, D. J., Mohamed, S., and Welling, M. Semi-supervised learning with deep generative models. In *Proceedings of the 27th International Conference on Neural Information Processing Systems - Volume 2, NIPS'14*, pp. 3581–3589, Cambridge, MA, USA, 2014. MIT Press.
- Kirkpatrick, J., Pascanu, R., Rabinowitz, N., Veness, J., Desjardins, G., Rusu, A. A., Milan, K., Quan, J., Ramalho, T., Grabska-Barwinska, A., et al. Overcoming catastrophic forgetting in neural networks. *Proceedings of the national academy of sciences*, 2017.
- Kosioerek, A., Kim, H., Teh, Y. W., and Posner, I. Sequential attend, infer, repeat: Generative modelling of moving objects. In Bengio, S., Wallach, H., Larochelle, H., Grauman, K., Cesa-Bianchi, N., and Garnett, R. (eds.), *Advances in Neural Information Processing Systems 31*, pp. 8606–8616. Curran Associates, Inc., 2018.
- Kosioerek, A., Sabour, S., Teh, Y. W., and Hinton, G. E. Stacked capsule autoencoders. In *Advances in Neural Information Processing Systems*, pp. 15486–15496, 2019.
- Kumaran, D., Hassabis, D., and McClelland, J. L. What learning systems do intelligent agents need? complementary learning systems theory updated. *Trends in cognitive sciences*, 20(7):512–534, 2016.
- Lecun, Y., Bottou, L., Bengio, Y., and Haffner, P. Gradient-based learning applied to document recognition. *Proceedings of the IEEE*, 86(11):2278–2324, Nov 1998. ISSN 0018-9219. doi: 10.1109/5.726791.
- Lee, D.-H. Pseudo-label : The simple and efficient semi-supervised learning method for deep neural networks. *ICML 2013 Workshop : Challenges in Representation Learning (WREPL)*, 07 2013.
- Li, Y., Wang, Y., Liu, Q., Bi, C., Jiang, X., and Sun, S. Incremental semi-supervised learning on streaming data. *Pattern Recognition*, 88, 11 2018. doi: 10.1016/j.patcog.2018.11.006.
- Li, Z. and Hoiem, D. Learning without forgetting. *IEEE transactions on pattern analysis and machine intelligence*, 40(12):2935–2947, 2017.

- Loo, H. R. and Marsono, M. N. Online data stream classification with incremental semi-supervised learning. In *Proceedings of the Second ACM IKDD Conference on Data Sciences*, CoDS '15, pp. 132–133, New York, NY, USA, 2015. Association for Computing Machinery. ISBN 9781450334365. doi: 10.1145/2732587.2732614.
- Lopez-Paz, D. and Ranzato, M. Gradient episodic memory for continual learning. In *Proceedings of the 31st International Conference on Neural Information Processing Systems*, NIPS'17, pp. 6470–6479, USA, 2017. Curran Associates Inc. ISBN 978-1-5108-6096-4.
- Miyato, T., Maeda, S.-i., Ishii, S., and Koyama, M. Virtual adversarial training: a regularization method for supervised and semi-supervised learning. *IEEE transactions on pattern analysis and machine intelligence*, 2018.
- Netzer, Y., Wang, T., Coates, A., Bissacco, A., Wu, B., and Ng, A. Y. Reading digits in natural images with unsupervised feature learning. In *NIPS Workshop on Deep Learning and Unsupervised Feature Learning 2011*, 2011.
- Oliver, A., Odena, A., Raffel, C. A., Cubuk, E. D., and Goodfellow, I. Realistic evaluation of deep semi-supervised learning algorithms. In *Advances in Neural Information Processing Systems*, pp. 3235–3246, 2018.
- Oord, A. v. d., Li, Y., and Vinyals, O. Representation learning with contrastive predictive coding. *arXiv preprint arXiv:1807.03748*, 2018.
- Pan, S. and Yang, Q. A Survey on Transfer Learning. *IEEE Transactions on Knowledge and Data Engineering*, 22(10):1345–1359, 2010.
- Parisi, G. I., Kemker, R., Part, J. L., Kanan, C., and Wermter, S. Continual lifelong learning with neural networks: A review. *Neural Networks*, 113:54 – 71, 2019. ISSN 0893-6080. doi: <https://doi.org/10.1016/j.neunet.2019.01.012>.
- Pehlevan, C., Genkin, A., and Chklovskii, D. B. A clustering neural network model of insect olfaction. In *2017 51st Asilomar Conference on Signals, Systems, and Computers*, pp. 593–600. IEEE, 2017.
- Rao, D., Visin, F., Rusu, A., Pascanu, R., Teh, Y. W., and Hadsell, R. Continual unsupervised representation learning. In *Advances in Neural Information Processing Systems 32*, pp. 7645–7655. Curran Associates, Inc., 2019.
- Rasmus, A., Berglund, M., Honkala, M., Valpola, H., and Raiko, T. Semi-supervised learning with ladder networks. In Cortes, C., Lawrence, N. D., Lee, D. D., Sugiyama, M., and Garnett, R. (eds.), *Advances in Neural Information Processing Systems 28*, pp. 3546–3554. Curran Associates, Inc., 2015.
- Rebuffi, S., Kolesnikov, A., Sperl, G., and Lampert, C. H. icarl: Incremental classifier and representation learning. In *2017 IEEE Conference on Computer Vision and Pattern Recognition, CVPR'17*, pp. 5533–5542, 2017.
- Ren, M., Triantafillou, E., Ravi, S., Snell, J., Swersky, K., Tenenbaum, J. B., Larochelle, H., and Zemel, R. S. Meta-learning for semi-supervised few-shot classification. In *Proceedings of 6th International Conference on Learning Representations ICLR*, 2018.
- Ruder, S. An overview of multi-task learning in deep neural networks. *arXiv preprint arXiv:1706.05098*, 2017.
- Rusu, A. A., Rabinowitz, N. C., Desjardins, G., Soyer, H., Kirkpatrick, J., Kavukcuoglu, K., Pascanu, R., and Hadsell, R. Progressive neural networks. *arXiv preprint arXiv:1606.04671*, 2016.
- Shin, H., Lee, J. K., Kim, J., and Kim, J. Continual learning with deep generative replay. In Guyon, I., Luxburg, U. V., Bengio, S., Wallach, H., Fergus, R., Vishwanathan, S., and Garnett, R. (eds.), *Advances in Neural Information Processing Systems 30*, pp. 2990–2999. Curran Associates, Inc., 2017.
- Snell, J., Swersky, K., and Zemel, R. Prototypical networks for few-shot learning. In *Advances in neural information processing systems*, pp. 4077–4087, 2017.
- Springenberg, J. T. Unsupervised and semi-supervised learning with categorical generative adversarial networks. *arXiv preprint arXiv:1511.06390*, 2015.
- Tarvainen, A. and Valpola, H. Mean teachers are better role models: Weight-averaged consistency targets improve semi-supervised deep learning results. In Guyon, I., Luxburg, U. V., Bengio, S., Wallach, H., Fergus, R., Vishwanathan, S., and Garnett, R. (eds.), *Advances in Neural Information Processing Systems 30*, pp. 1195–1204. Curran Associates, Inc., 2017.
- Tschannen, M., Bachem, O., and Lucic, M. Recent advances in autoencoder-based representation learning. *arXiv preprint arXiv:1812.05069*, 2018.
- van de Ven, G. M. and Tolias, A. S. Three scenarios for continual learning. *arXiv preprint arXiv:1904.07734*, 2019.
- Venkatesan, R. and Er, M. J. A novel progressive learning technique for multi-class classification. *Neurocomput.*, 207(C):310–321, September 2016. ISSN 0925-2312. doi: 10.1016/j.neucom.2016.05.006.
- Watanabe, T., Náñez, J. E., and Sasaki, Y. Perceptual learning without perception. *Nature*, 413(6858):844, 2001.

- Xie, J., Girshick, R., and Farhadi, A. Unsupervised deep embedding for clustering analysis. In Balcan, M. F. and Weinberger, K. Q. (eds.), *Proceedings of The 33rd International Conference on Machine Learning*, volume 48 of *Proceedings of Machine Learning Research*, pp. 478–487, New York, New York, USA, 20–22 Jun 2016. PMLR.
- Yang, J., Parikh, D., and Batra, D. Joint unsupervised learning of deep representations and image clusters. In *Proceedings of the IEEE Conference on Computer Vision and Pattern Recognition*, pp. 5147–5156, 2016.
- Yoon, J., Yang, E., Lee, J., and Hwang, S. J. Lifelong learning with dynamically expandable networks. In *International Conference on Learning Representations*, 2018.
- Yosinski, J., Clune, J., Bengio, Y., and Lipson, H. How transferable are features in deep neural networks? In Ghahramani, Z., Welling, M., Cortes, C., Lawrence, N. D., and Weinberger, K. Q. (eds.), *Advances in Neural Information Processing Systems 27*, pp. 3320–3328. Curran Associates, Inc., 2014.
- Zenke, F., Poole, B., and Ganguli, S. Continual learning through synaptic intelligence. In *International Conference on Machine Learning*, 2017.
- Zeno, C., Golan, I., Hoffer, E., and Soudry, D. Task agnostic continual learning using online variational bayes. *arXiv preprint arXiv:1803.10123*, 2018.
- Zhou, G., Sohn, K., and Lee, H. Online incremental feature learning with denoising autoencoders. In Lawrence, N. D. and Girolami, M. (eds.), *Proceedings of the Fifteenth International Conference on Artificial Intelligence and Statistics*, volume 22 of *Proceedings of Machine Learning Research*, pp. 1453–1461, La Palma, Canary Islands, 21–23 Apr 2012. PMLR.

## SUPPLEMENTARY MATERIAL

### A. STAM Notation and Hyperparameters

All STAM notation and parameters are listed in Tables 1-4.

### B. Baseline architectures

The details of the CAE architecture are given in Table 5. FC denotes fully connected layers, and Conv.Trans denotes transposed convolution layers. The RotNet architecture is as described in (Gidaris et al., 2018).

### C. A closer look at STAM in Incremental UPL

We refer the reader to Figure 7. As we introduce new classes to the incremental UPL stream, the architecture recognizes previously learned classes without any major degradation in classification accuracy (left column). The average accuracy per phase is decreasing, which is due to the increasingly difficult expanding classification task. For EMNIST, we only show the average accuracy because there are 47 total classes. In all datasets, we observe that layer-3 (corresponding to the largest receptive field) contains the highest fraction of CIN centroids (center column). The ability to recognize new classes is perhaps best visualized in the LTM centroid count (right column). During each phase the LTM count stabilizes until a sharp spike occurs at the start of the next phase when new classes are introduced. This reinforces the claim that the LTM pool of centroids (i) is stable when there are no new classes, and (ii) is able to recognize new classes via novelty detection when they appear. In the EMNIST experiment, as the number of classes increases towards 47, we gradually see fewer “spikes” in the LTM centroids for the lower receptive fields, which is expected given the repetition of patterns at that small patch size. However, the highly CIN layer-3 continues to recognize new classes and create centroids, even when the last few classes are introduced.

### D. Effect of unlabeled and labeled data on STAM

We next examine the effects of unlabeled and labeled data on the STAM architecture (Figure 8). As we vary the length of the unlabeled data stream (left), we see that STAMs can actually perform well even with much less unlabeled data. This suggests that the STAM architecture may be applicable even where the datastream is much shorter than in the experiments of this paper. A longer stream would be needed however if there are many classes and some of them are infrequent. The accuracy “saturation” observed by increasing the unlabeled data from 20000 to 60000 can be explained based on the memory mechanism, which does

not update centroids after they move to LTM. As showed in the ablation studies, this is necessary to avoid forgetting classes that no longer appear in the stream. The effect of varying the number of labeled examples per class (right) is much more pronounced. We see that the STAM architecture can perform well above chance even in the extreme case of only a single (or small handful of) labeled examples per class.

### E. STAM Hyperparameter Sweeps

We examine the effects of STAM hyperparameters in Figure 9. (a) As we decrease the rate of  $\alpha$ , we see a degradation in performance. This is likely due to the static nature of the LTM centroids - with low  $\alpha$  values, the LTM centroids will primarily represent the patch they were initialized as. (b) As we vary the rates of  $\gamma$ , there is little difference in our final classification rates. This suggests that the maximum  $g_{l,j}(k)$  values are quite high, which may not be the case in other datasets besides SVHN. (c) We observe that STAM is robust to changes in  $\Theta$ . (d,e) The STM size  $\Delta$  has a major effect on the number of learned LTM centroids and on classification accuracy. (e) The accuracy in phase-5 for different numbers of layer-3 LTM centroids (and corresponding  $\Delta$  values). The accuracy shows diminishing returns after we have about 1000 LTM centroids at layer-3. (g,h) As  $\beta$  increases the number of LTM centroids increases (due to a lower rate of novelty detection); if  $\beta \geq 0.9$  the classification accuracy is about the same.

### F. Uniform UPL

In order to examine if the STAM architecture can learn all classes simultaneously, but without knowing how many classes exist, we also evaluate the STAM architecture in a uniform UPL scenario (Figure 10). Note that LTM centroids converge to a constant value, at least at the top layer. Each class is recognized at a different level of accuracy, depending on the similarity between that class and others.

### G. Image preprocessing

Given that each STAM operates on individual image patches, we perform *patch normalization* rather than image normalization. We chose a normalization operation that helps to identify similar patterns despite variations in the brightness and contrast: every patch is transformed to zero-mean, unit variance before clustering. At least for the datasets we consider in this paper, grayscale images result in higher classification accuracy than color.

We have also experimented with ZCA whitening and Sobel filtering. ZCA whitening did not work well because it requires estimating a transformation from an entire image

dataset (and so it is not compatible with the online nature of the UPL problem). Sobel filtering did not work well because STAM clustering works better with filled shapes rather than the fine edges produced by Sobel filters.

## H. Memory footprint analysis

The memory requirement of the STAM model can be calculated as:

$$M = \sum_{l=1}^{\Lambda} \rho_l^2 \cdot (|C_l| + \Delta) \quad (8)$$

For the 3-layer SVHN architecture with  $|C_l| \approx 3000$  LTM centroids in every layer and  $\Delta = 2000$ , the memory footprint is 5,064,000 pixels, equivalent to roughly 5000 grayscale SVHN digits. This memory requirement can be significantly reduced however. Figure 9(f) shows that the accuracy remains almost the same when  $\Delta = 500$  and  $|C_l| \approx 1000$ . With these values the memory footprint reduces to about 950,000 pixels, equivalent to roughly 930 grayscale SVHN digits.

By comparison, the CAE architecture has 4,683,425 trainable parameters, which should be stored at floating-point precision. With four bytes per weight, then STAM model would require  $\frac{950000}{4683425 \times 4} \approx 5\%$  of the CAE's memory footprint. Future work can decrease the STAM memory requirement further by merging similar LTM centroids.

Table 1. STAM Notation

Symbol	Description
$\mathbf{x}$	input vector.
$n$	dimensionality of input data
$M_l$	number of patches at layer $l$ (index: $m = 1 \dots M_l$ )
$\mathbf{x}_{l,m}$	$m$ 'th input patch at layer $l$
$C_l$	set of centroids at layer $l$
$\mathbf{c}_{l,j}$	centroid $j$ at layer $l$
$d(\mathbf{x}, c)$	distance between an input vector $\mathbf{x}$ and a centroid $c$
$\hat{c}(\mathbf{x})$	index of nearest centroid for input $x$
$\tilde{d}_l$	novelty detection distance threshold at layer $l$
$U(t)$	the set of classes seen in the unlabeled data stream up to time $t$
$L(t)$	the set of classes seen in the labeled data up to time $t$
$k$	index for representing a class
$g_{l,j}(k)$	association between centroid $j$ at layer $l$ and class $k$ .
$\bar{D}_l$	average distance between a patch and its nearest neighbor centroid at layer $l$ .
$v_{l,m}(k)$	vote of patch $m$ at layer $l$ for class $k$
$v_l(k)$	vote of layer $l$ for class $k$
$k(\mathbf{x})$	true class label of input $x$
$\hat{k}(\mathbf{x})$	inferred class label of input $x$
$\Phi(\mathbf{x})$	embedding vector of input $x$

Table 2. STAM Hyperparameters

Symbol	Default	Description
$\Lambda$	3	number of layers (index: $l = 1 \dots \Lambda$ )
$\alpha$	0.1	centroid learning rate
$\beta$	0.95	percentile for novelty detection distance threshold
$\gamma$	0.15	used in definition of class informative centroids
$\Delta$	see below	STM capacity
$\theta$	30	number of updates for memory consolidation
$\rho_l$	see below	patch dimension

Table 3. MNIST/EMNIST Architecture

Layer	$\rho_l$	$\Delta$ (incremental)	$\Delta$ (uniform)
1	8	400	2000
2	13	400	2000
3	20	400	2000

Table 4. SVHN Architecture

Layer	$\rho_l$	$\Delta$ (incremental)	$\Delta$ (uniform)
1	10	2000	10000
2	14	2000	10000
3	18	2000	10000

Table 5. CAE Architecture

Encoder					
Layer Type	# Filters	Kernel Size	Stride	# Units	Activation Unit
Conv	128	3	1	-	ReLu
Conv	64	3	2	-	ReLu
Conv	32	3	2	-	ReLu
FC	-	-	-	1568	ReLu
FC	-	-	-	64	Sigmoid
Decoder					
Layer Type	# Filters	Kernel Size	Stride	# Units	Activation Unit
FC	-	-	-	1568	ReLu
Conv_Trans	128	3	1	-	ReLu
Conv_Trans	64	3	2	-	ReLu
Conv_Trans	32	3	2	-	ReLu
Conv_Trans	1	1	1	-	Linear

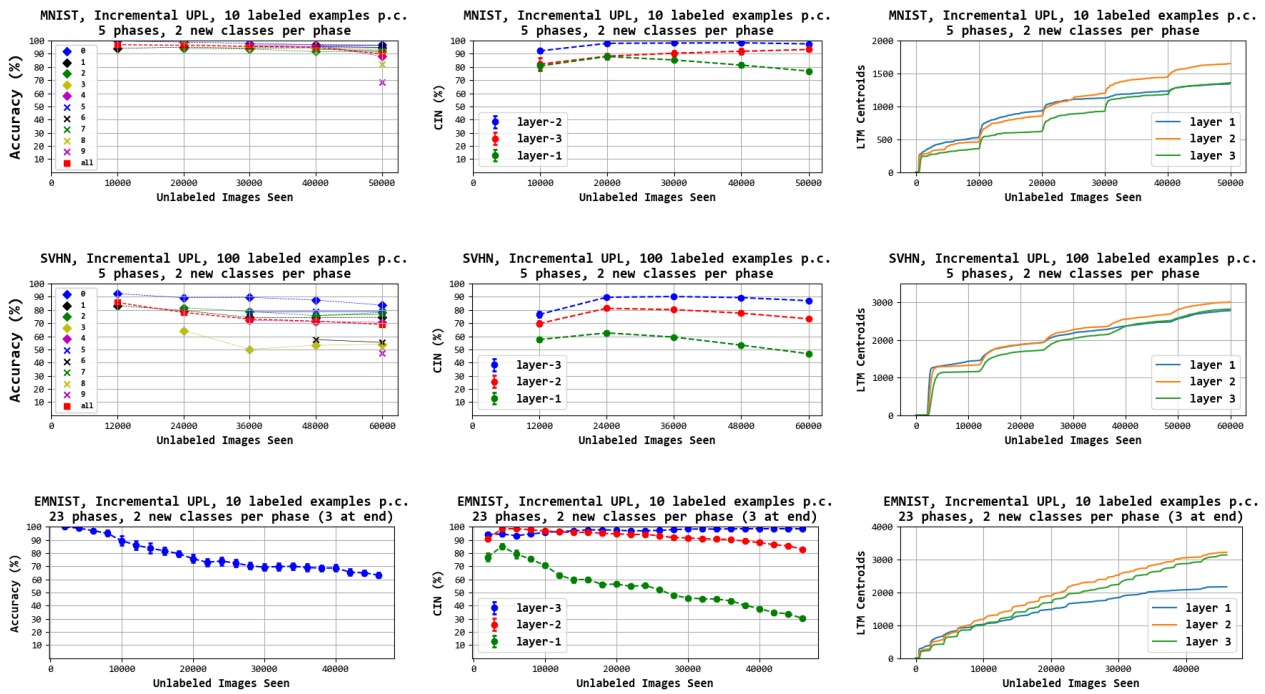


Figure 7. STAM Incremental UPL evaluation for MNIST (row-1), SVHN (row-2), and EMNIST (row-3). Per-class and average classification accuracy (left); number of LTM centroids over time (center); fraction of CIN centroids over time (right). The task is expanding classification, i.e., recognize all classes seen so far.

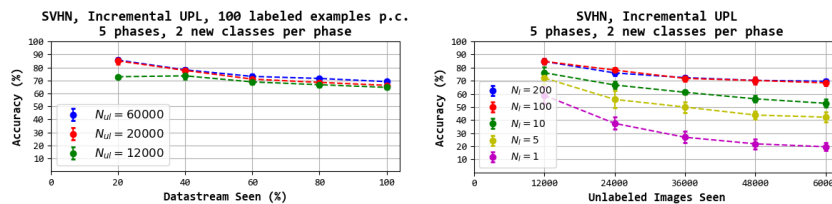
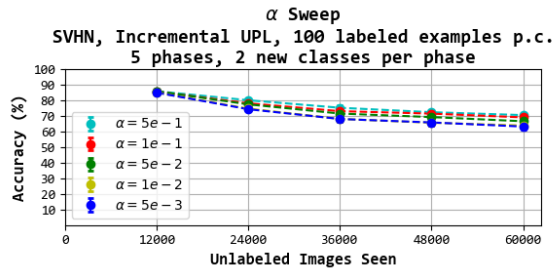
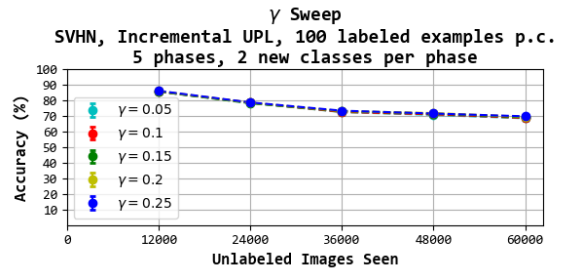


Figure 8. The effect of varying the amount of unlabeled data in the entire stream (left) and labeled data per class (right).

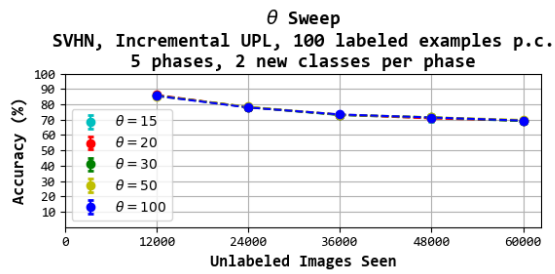




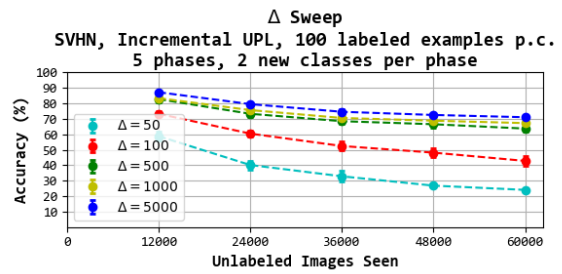
(a)



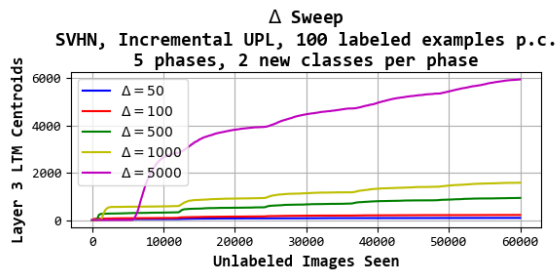
(b)



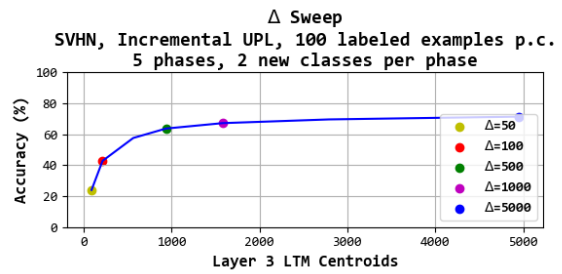
(c)



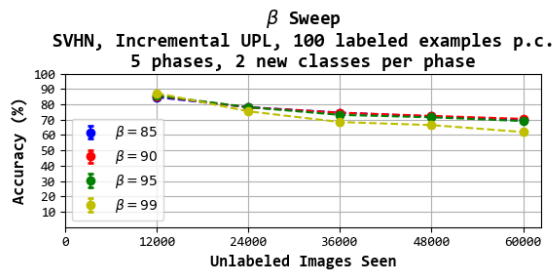
(d)



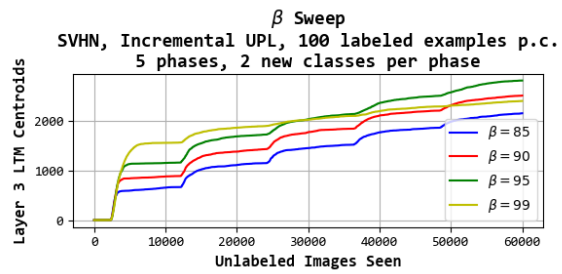
(e)



(f)



(g)



(h)

Figure 9. Hyperparameter sweeps for  $\alpha$ ,  $\gamma$ ,  $\theta$ ,  $\beta$ , and  $\Delta$ .

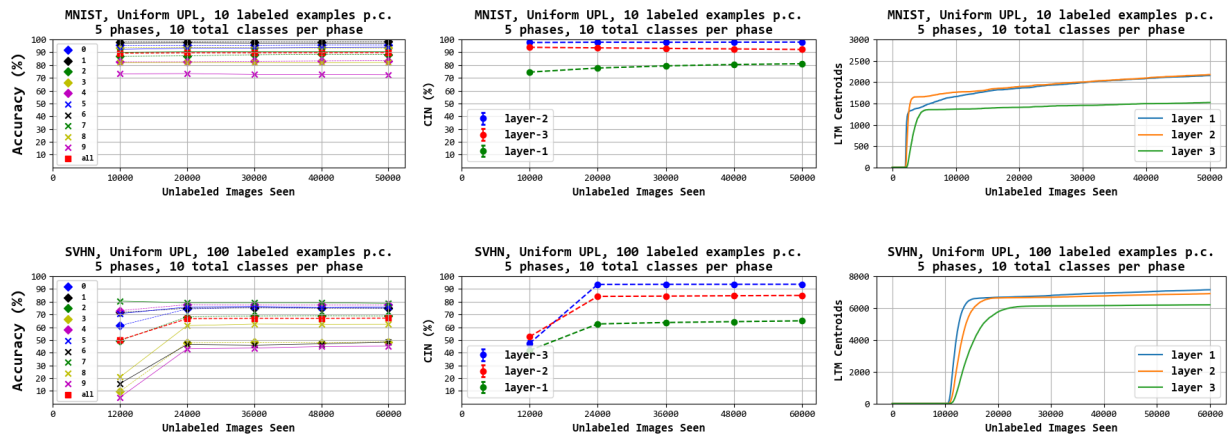


Figure 10. Uniform UPL evaluation for MNIST (row-1) and SVHN (row-2). Per-class/average classification accuracy is given at the left; the number of LTM centroids over time is given at the center; the fraction of CIN centroids over time is given at the right.